MRI Brain Tumor Segmentation and Patient Survival Prediction Using Random Forests and Fully Convolutional Networks

Mohammadreza Soltaninejad[1(✉)], Lei Zhang[1], Tryphon Lambrou[1], Guang Yang[2], Nigel Allinson[1], and Xujiong Ye[1]

[1] Laboratory of Vision Engineering, School of Computer Science, University of Lincoln, Lincoln, UK
{msoltaninejad,lzhang,tlambrou,nallinson,xye}@lincoln.ac.uk
[2] National Heart and Lung Institute, Imperial College London, London, UK
g.yang@imperial.ac.uk

Abstract. In this paper, we propose a learning based method for automated segmentation of brain tumor in multimodal MRI images, which incorporates two sets of machine-learned and hand-crafted features. Fully convolutional networks (FCN) forms the machine-learned features and texton based histograms are considered as hand-crafted features. Random forest (RF) is used to classify the MRI image voxels into normal brain tissues and different parts of tumors. The volumetric features from the segmented tumor tissues and patient age applying to an RF is used to predict the survival time. The method was evaluated on MICCAI-BRATS 2017 challenge dataset. The mean Dice overlap measures for segmentation of validation dataset are 0.86, 0.78 and 0.66 for whole tumor, core and enhancing tumor, respectively. The validation Hausdorff values are 7.61, 8.70 and 3.76. For the survival prediction task, the classification accuracy, pairwise mean square error and Spearman rank are 0.485, 198749 and 0.334, respectively.

Keywords: Fully convolutional networks · Random forest
Deep learning · Texton · MRI · Brain tumor segmentation

1 Introduction

Delineation of the tumor boundary and assessment of tumor size are needed for patient management in terms of treatment planning [1] and monitoring treatment response [2], and current guidelines incorporate the use of Magnetic Resonance Images (MRI) [3,4]. Tumor assessment requires accurate full 3D volume measurement of the tumor. However, automated segmentation of brain tumors is a very challenging task due to their high variation in size, shape and appearance (e.g. image uniformity and texture) [5].

Most of the classification-based brain tumor segmentation techniques used hand-crafted features which are fed into a classifier such as random forests

A. Crimi et al. (Eds.): BrainLes 2017, LNCS 10670, pp. 204–215, 2018.
https://doi.org/10.1007/978-3-319-75238-9_18

(RF), support vector machines, etc. [6,7]. Among the conventional classifiers, RF presents the best segmentation results [7,8]. However, one limitation of these types of methods is that a large number of features are required in order to provide better description of the different types of classes (tissues) in the images. Therefore, they result in a high dimensional problem which makes the process more complicated and time consuming.

Due to the recent advances in deep convolutional neural networks (CNNs) they have been widely used for recognition of the patterns in the images. Several CNN-based methods have been developed for medical image analysis, especially for segmentation of brain tumors in MRI [9–11].

Recently, fully convolutional networks (FCN) have been suggested for dense (i.e. per-pixel) classification with the advantage of end-to-end learning [12]. Despite the advantage of dense pixel classification, FCN-based methods still have limitations of considering the local dependencies in higher resolution (pixel) level. The loss of spatial information, which occurs in the pooling layers, results in coarse segmentation. This limitation will be addressed in this paper by incorporating high resolution hand-crafted textural features which consider local dependencies of the pixel. Texton feature maps [13] provides significant information on multi-resolution image patterns in both spatial and frequency domains. This is an inspiration to combine texton features to a partially end-to-end learning process in order to improve the segmentation.

In this paper, a novel fully automatic learning based segmentation method is proposed, by applying hand-crafted and machine-learned features to an RF classifier. The machine-learned FCN based features detect the coarse region of the tumor while the hand-crafted texton descriptors consider the spatial features and local dependencies to improve the accuracy for segmentation of tumor tissue subtypes. Also, the survival time of the patients is predicted using the volumetric features extracted from the segmented images and the patient information (in this paper, age).

2 Methods

The proposed segmentation method is comprised of four major steps (preprocessing, CNN design, Texton map extraction, RF classifier) that are depicted in Fig. 1.

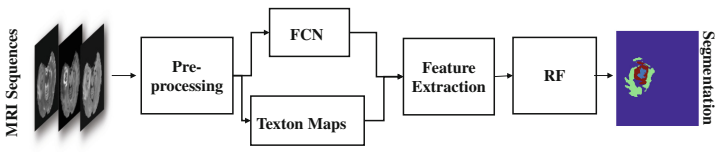

Fig. 1. The overall flowchart of the proposed method which uses hand-designed and machine-learned features for automatic brain tumor segmentation in MRI images.

2.1 Preprocessing

Firstly, the 1% highest and lowest intensity values for each image are eliminated. The 1% highest values correspond to the hyper intensities of the remaining voxels related to the skull, and the 1% lowest values correspond to the elimination of the background noise. The intensities were normalized for each protocol by subtracting the average of intensities of the image and dividing by their standard deviation. Then, the histogram of each image was normalized and matched to the one of the patient images which is selected as the reference. The normalization procedure for each individual protocol is illustrated in Fig. 2. To eliminate the bias of the matched histogram to the reference case, another block ("Histogram Matching 2" in Fig. 2.) is added to the process according to [14]. In this procedure, the average of all the new histograms including the initial reference case is calculated for each protocol and the histograms are again matched to the new reference, i.e. the average histogram for each protocol. In the second stage, for each case, the intensities of new images of all the protocols obtained from the first step are linearly normalized to the range [0, 255]. The protocols that are used in this study are Fluid Attenuated Inversion Recovery (FLAIR), post-contrast T1-weighted (T1-contrast), and T2-weighted.

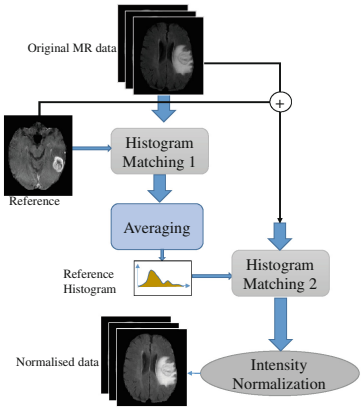

Fig. 2. Flowchart of the multimodal normalization and histogram matching of the MR dataset for one protocol.

2.2 Feature Extraction Form the FCN Layers

The FCN network is modified by eliminating the final classifier layer and converting all the fully connected (FC) layers to convolution layers (CONVs). This is realized by adding a CONV of size 1×1 with channel dimension 4 (i.e. number of output classes). A deconvolution layer is added to upsample the coarse output bilinearly to predict the scores for each pixels of multimodal MRI images that provides the pixel-wise fine segmentation.

The output stride is divided in half by predicting from a 16-pixel stride layer. A 1×1 convolution is added to the *POOL4* to further predict the classes. The corresponding output is combined with the output of *CONV7* at stride 32 by adding a 2x upsampling layer. The upsampling layer is initially a bilinear interpolation and its parameters can be learned later. The stride 16 predictions are then upsampled back to the image. This structure is called FCN-16.

The same procedure is applied on the *POOL3*, the predictions at 8 stride is then combined with the 2x upsampling of the combinations of the predictions derived from stride 16 and 32 that results in FCN-8s architecture. The FCN-8s provides relatively finer segmentation compared with the FCN-16s. In the same way, to produce finer predictions, we could decrease the strides of the pooling layers. However, it makes network training inefficient, since such implementation will increase the computational cost and increase the network convergence time.

The architecture of FCN based on VGG16 [15] for brain tumor segmentation is presented in Fig. 3. The predictions at shallow layers are produced using a skip layer that combines coarse predictions at deep layers to improve segmentation details.

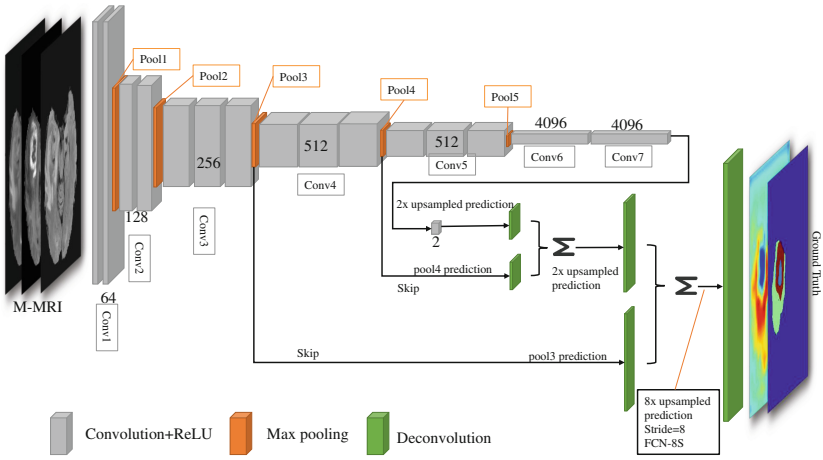

Fig. 3. The detailed architecture of the FCN used for segmentation of brain tumor in multimodal MRI.

The VGG model is designed based on natural image with intensities with bit depth = 8 (i.e. the intensity range is [0, 255]). The VGG model has also the capability of being further trained by adding more datasets to the existing pre-trained model. The initialization using a pre-trained model decreases the training time. Furthermore, the shallower layer of any CNNs learn more common features of images which are more likely domain-independent, thus such features could be used among different kinds of images. In this case, a pre-trained model could improve the model accuracy for new images. In order to use the pre-trained

VGG16 model for the case of medical MR images, some modifications should be taken into account. The intensities of the images are normalized into the range of a natural image which is [0, 255]. The pre-trained VGG model is trained on RGB images which has three channels. Therefore, three protocols were selected to build the input data, i.e. FLAIR, T1-contrast and T2-weighted according to the annotation protocol described in [8]. T2-weighted was selected since it was used mainly to segment the "edema". FLAIR was used to discriminate the edema from ventricles and fluid-filled structures. T1-contrast was utilized to distin-guish other tumor subtypes. The "enhancing tumor" appears as hyper-intensities and the "necrosis" appears as low intensities within the enhancing borders in T1-contrast.

The feature vector is generated for each voxel based on the score map from the FCN. For each class label, a score map is generated. Overall, 4 maps are generated using the standard MICCAI-BRATS17 labelling system, i.e. background plus normal brain, necrosis plus non-enhancing, edema, and enhancing tumor. The values of each map layer corresponding to each voxel are considered as machine-learned features of that voxel.

2.3 Spatial Feature Extraction Using Textons

The coarse results of the FCN-based segmentation are due to the down-sampling that occurs in the pooling layers. Given that the local dependency is not sufficiently considered in the FCN, a new pipeline using texton based feature descriptor derived from the convolutional operator is proposed. Textons are used since they are powerful feature descriptors that represent the local dependencies and neighborhood system information in all phases, i.e. convolution, k-means clustering and histogram calculation. Textons are obtained by convolving the image with a Gabor filter bank. To cover all orientations six different filter directions were used: [0°, 30°, 45°, 60°, 90°, 120°]. Filter sizes were [0.3, 0.6, 0.9, 1.2, 1.5] and the wavelength of sinusoid coefficients of the Gabor filters were [0.8, 1.0, 1.2, 1.5].

The MR images are convolved with the Gabor filters, then the filter responses are merged together and clustered using k-means clustering. The number of clusters 16 was selected as the optimum value for the number of clusters in texton map. The texton map is created by assigning the cluster number to each voxel of the image.

Each pixel in the image is described by its intensity and neighborhood pixels. For each pixel, its neighborhood with size $n \times n$ pixel is represented by the histogram of texton while the center pixel is represented by its normalized intensity. This descriptor of each pixel implicitly encodes the information that the center pixel conditionally depends on its neighborhood, thus incorporates the local dependencies into feature representation. The texton histogram is a vector with the size of k-means clusters (i.e. 16 in this paper). The procedure of mapping the connectivity based on the texton IDs (in the neighborhood window) to the histogram is illustrated in Fig. 4. The texton feature for each voxel is the histogram of textons in a neighborhood window of 5×5 around that voxel.

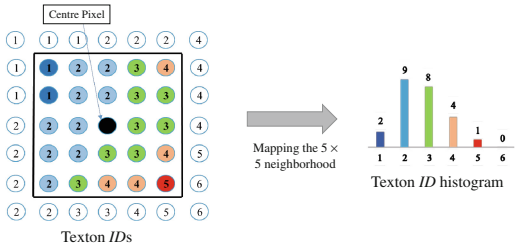

Fig. 4. The connectivity of the adjacent pixels from the histogram of the texton *ID*s in a 5×5 neighborhood of the center pixel. The texton clusters are integers in the range [1, 16]. This is a simplified example and the texton histogram values are zero for *ID*s from 6 to 16.

Figure 5 shows the FCN based score maps for each class layer and the protocols used to generate the corresponding score maps. Figure 5 also shows the corresponding texton maps.

It should be noted that the histogram of texton is considered for the adjacent pixels in the neighborhood and the target pixel (in the center) is not counted. Therefore, the normalized intensity value of the voxels in each protocol which is obtained from the preprocessing stage is also included in the feature vector. In total, 55 features were collected (4 FCN score maps, 3 protocol intensities and 48 texton histograms from three protocols) for usage in the classification stage. Figure 6 shows a graphic presentation of feature vector generation and presents how machine-learned and hand-designed features are integrated together.

2.4 Random Forest Classification

The potential tumor area detected by the FCN output was considered as the initial region of interest (ROI). This ROI was selected as a confidence margin of 10 voxels in 3D space around the detected initial tumor area which was calculated by morphological dilation. The feature vectors for voxels in this ROI were fed to an RF [16]. The main parameters in designing RF are tree depth and the number of trees. RF parameters were tuned by examining different tree depths and number of trees on training datasets and evaluating the classification accuracy using 5-fold cross validation. The number of 50 trees with depth 15 provided an optimum generalization and accuracy. Based on the classes assigned for each voxel in the validation dataset, the final segmentation mask was created by mapping back the voxel estimated class to the segmentation mask volume. Finally, the bright regions in the healthy part of the brain near to the skull were eliminated using a connected component analysis.

2.5 Patient Overall Survival Prediction

A new task is introduced in MICCAI-BRATS 2017 challenge which is prediction of patients' overall survival (OS) from the pre-operative scans. The features

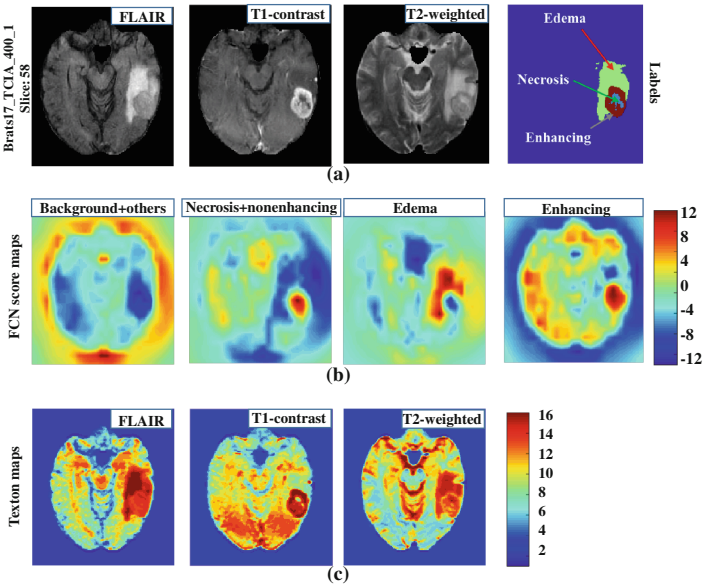

Fig. 5. The FCN-based score maps and texton maps generated from the multimodal MRI protocols: FLAIR, T1-contrast and T2-weighted. (a) The original images and the corresponding brain tissue labels, (b) FCN score maps generated from all three protocols together for each individual class, (c) texton maps generated from each individual protocol.

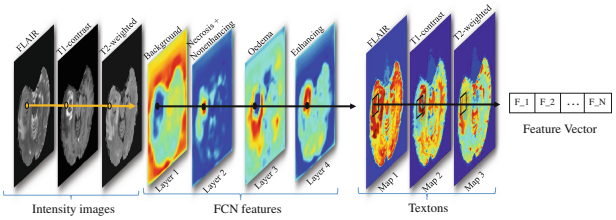

Fig. 6. The details of feature vector generation for the hybrid method. Machine based features from FCN are extracted based on pixel and the hand-designed texton features extracted from the neighborhood around the pixel and considers the local dependencies.

which are used for this task are the relative volume size of each tumor subtype after segmentation. The number of voxels within each segmented volume related to each tumor is divided by the total number of voxels within the brain. The age of patients is considered as another feature. Since RF can handle the categorical data and features with different ranges and they present promising classification and regression tasks, they are used for the prediction of survival time. An RF with the number of 1000 trees and with depth 15 is used as a regression model.

3 Results

The experiments were implemented on a PC with CPU Intel Core i7 and RAM 16 GB with the operating system windows 8.1. GPU GeForce gtx980i was used for reducing the training time of the FCN. The FCN was implemented using MatCovNet toolbox [17]. The VGG16 network was implemented using the Caffe model [18]. The network weights were initialized using pre-trained VGG16 model. The mini-batch stochastic gradient descent (SGD) with momentum was employed to train the FCN. The learning rate and momentum were set to 0.0001 and 0.9, respectively. The batch size was set to 20 and the total number of 150 epochs were used. The dropper layers with the rate of 0.5 were used to reduce overfitting. Other sections of the proposed method were performed using MATLAB 2016b. RF open source code provided in [19], which is a specialized toolbox for RF classification based on MATLAB, was utilized for the classification.

3.1 Segmentation Task

Both FCN and RF were trained on BRATS 2017 [8,20–22] training dataset which include 220 high grade glioma (HGG) and 75 low grade glioma (LGG) patient cases. The method was evaluated on BRTAS 2017 validation (46 patient cases) and testing (146 patient cases) datasets.

The evaluation measures which are provided by the CBICA's Image Processing Portal (IPP) [23], i.e. Dice score, sensitivity, specificity, Hausdorff distance, were used to compare the segmentation results with the gold standard (blind testing). Figure 7 shows segmentation results of the proposed method on some cases of BRATS 2017 validation and testing datasets. The segmentation results of using only FCN are also shown in Fig. 7(c) to provide a comparison between both methods. As can be seen in Fig. 7(d), the proposed method provides finer segmentations compared to FCN only segmentation (Fig. 7(c)).

Table 1 provides the evaluation results obtained by applying the proposed method on BRATS 2017 validation dataset. The results of this paper appear as the team name "LoVE" on the CBICA portal leaderboard [24]. Table 2 provides the evaluation results for the testing dataset. It should be noted that only Dice and Hausdorff measures were provided by the challenge organizers at the time of submission of this paper. The mean Dice overlap measures for segmentation of validation dataset against ground truth are 0.86, 0.78 and 0.66 for the whole tumor, core and enhancing tumor, respectively. The corresponding Dice score results for the testing dataset are 0.85, 0.69 and 0.67, respectively. The average Hausdorff distance for segmentation of validation dataset against ground truth is for 7.61, 8.70 and 3.76 for the whole tumor, core and enhancing tumor, respectively. The corresponding Hausdorff distances for the testing dataset are 6.12, 28.72 and 23.55, respectively.

3.2 Survival Prediction Task

The training dataset includes 163 patients provided with overall survival time and the age of patients. The validation and test datasets include 33 and 95

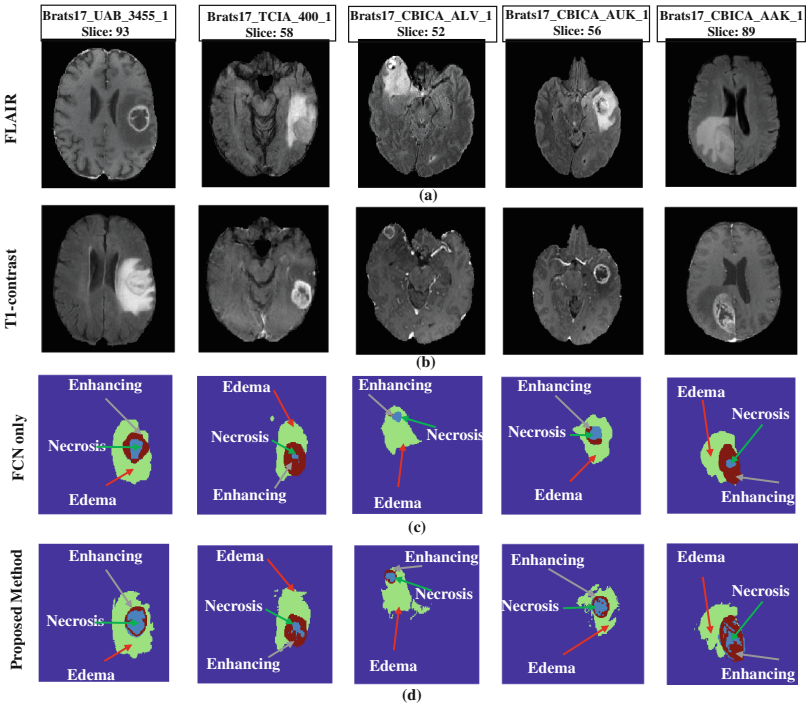

Fig. 7. Segmentation masks for some validation and test datasets, using the proposed method. The case names and the slice number are mentioned on the top of the images. (a) FLAIR images, (b) T1-contrast images, (c) segmentation masks and labels using FCN only, (d) segmentation masks and labels using the proposed method.

Table 1. Segmentation results for validation dataset which was provided by CBICA portal. ET: enhancing tumor, WT: whole tumor, TC: tumor core.

	Dice			Sensitivity			Specificity			Hausdorff (95%)		
	ET	WT	TC	ET	WT	TC	ET	WT	TC	ET	WT	TC
Mean	0.66	0.86	0.78	0.57	0.83	0.72	1.00	1.00	1.00	3.76	7.61	8.70
STD	0.28	0.09	0.19	0.28	0.13	0.21	0.00	0.01	0.00	4.38	12.99	13.52
Median	0.73	0.90	0.88	0.61	0.88	0.82	1.00	1.00	1.00	3.00	3.00	3.19
25 quantile	0.60	0.86	0.83	0.43	0.81	0.75	1.00	0.99	1.00	1.93	2.18	2.24
75 quantile	0.84	0.93	0.90	0.74	0.92	0.87	1.00	1.00	1.00	3.81	5.17	6.10

patients, respectively. For the evaluation on the training dataset, a 5-fold cross-validation was used. Then the RF was trained using all the training dataset and evaluated on the validation and testing datasets. The results were uploaded and the evaluation reports were provided by the CBICA system. Two evaluation procedures were considered based on classification and regression. In the

Table 2. Segmentation results for the test dataset (provided by CBICA portal).

	Dice			Hausdorff (95%)		
	ET	WT	TC	ET	WT	TC
Mean	0.67	0.85	0.69	23.55	6.12	28.72
STD	0.29	0.13	0.26	79.41	7.75	83.75
Median	0.76	0.89	0.80	2.83	4.12	6.63
25 quantile	0.57	0.81	0.60	1.41	3.00	4.12
75 quantile	0.86	0.92	0.87	6.85	5.87	12.20

Table 3. Survival prediction results for training, validation and test dataset.

Dataset	Accuracy	MSE	Median SE	STD SE	Spearman rank
Training	0.638	54063.061	17689	131754.325	0.809
Validation	0.485	198749.091	25921	480095.255	0.334
Testing	0.411	235546.432	45796	745532.757	0.389

classification scheme, the data were provided in three groups, i.e. long (more than 15 months), short (less than 10 months) and mid-survival (between, 10 and 15 months). Then the results were evaluated using accuracy of classification. In the regression scheme, the pairwise mean square error (MSE), median SE, standard deviation of SE, and Spearman rank were used. The corresponding results for all dataset types are provided in Table 3. The classification accuracy values are 0.638, 0.485, and 0.411 for training, validation, and testing datasets, respectively. The corresponding Spearman rank values are 0.809, 0.334, and 0.389, respectively.

4 Conclusion

In this paper, a novel method was proposed in which the machine-learned features extracted using FCN were combined with hand-crafted texton features to encode global information and local dependencies into feature representation. The score map with pixel-wise predictions was used as a feature map which was learned from multimodal MICCAI-BRATS 2017 training dataset using the FCN. The machine-learned features, along with hand-crafted texton features were then applied to random forests to classify each MRI image voxel.

The proposed method was tested on two independent MICCAI-BRATS 2017 challenge datasets, i.e. validation and testing, by uploading the results on the CBICA IPP portal and getting the evaluation results from the provided system (blind test). The results of the FCN based method showed that the application of the RF classifier to multimodal MRI images using machine-learned features based on FCN and hand-crafted features based on textons provides promising segmentations. The Dice overlap measure for the whole tumor was obtained 0.86

and 0.85 for validation and testing dataset, with the Hausdorff distances of 7.61 and 6.21, respectively.

The patient overall survival prediction task was performed with a regression based RF. The classification accuracy and regression evaluation were reported. The classification accuracy values of 0.638, 0.485, and 0.411 were obtained for training, validation, and testing datasets, respectively.

References

1. Gordillo, N., Montseny, E., Sobrevilla, P.: State of the art survey on MRI brain tumor segmentation. Magn. Reson. Imaging **31**, 1426–1438 (2013)
2. Eisele, S.C., Wen, P.Y., Lee, E.Q.: Assessment of brain tumor response: RANO and its offspring. Curr. Treat. Options Oncol. **17**, 35 (2016)
3. Wen, P.Y., Macdonald, D.R., Reardon, D.A., Cloughesy, T.F., Sorensen, A.G., Galanis, E., DeGroot, J., Wick, W., Gilbert, M.R., Lassman, A.B., Tsien, C., Mikkelsen, T., Wong, E.T., Chamberlain, M.C., Stupp, R., Lamborn, K.R., Vogelbaum, M.A., van den Bent, M.J., Chang, S.M.: Updated response assessment criteria for high-grade gliomas: response assessment in neuro-oncology working group. JCO **28**, 1963–1972 (2010)
4. Niyazi, M., Brada, M., Chalmers, A.J., Combs, S.E., Erridge, S.C., Fiorentino, A., Grosu, A.L., Lagerwaard, F.J., Minniti, G., Mirimanoff, R.O., Ricardi, U., Short, S.C., Weber, D.C., Belka, C.: ESTRO-ACROP guideline "target delineation of glioblastomas". Radiother Oncol. **118**, 35–42 (2016)
5. Patel, M.R., Tse, V.: Diagnosis and staging of brain tumors. Semin. Roentgenol. **39**, 347–360 (2004)
6. Pinto, A., Pereira, S., Correia, H., Oliveira, J., Rasteiro, D.M.L.D., Silva, C.A.: Brain tumour segmentation based on extremely randomized forest with high-level features. In: 2015 37th Annual International Conference of the IEEE Engineering in Medicine and Biology Society (EMBC), pp. 3037–3040 (2015)
7. Gotz, M., Weber, C., Blocher, J., Stieltjes, B., Meinzer, H., Maier-Hein, K.: Extremely randomized trees based brain tumor segmentation. In: Proceeding of BRATS Challenge-MICCAI, pp. 006–011 (2014)
8. Menze, B.H., Jakab, A., Bauer, S., Kalpathy-Cramer, J., Farahani, K., Kirby, J., Burren, Y., Porz, N., Slotboom, J., Wiest, R., Lanczi, L., Gerstner, E., Weber, M.A., Arbel, T., Avants, B.B., Ayache, N., Buendia, P., Collins, D.L., Cordier, N., Corso, J.J., Criminisi, A., Das, T., Delingette, H., Demiralp, Ç., Durst, C.R., Dojat, M., Doyle, S., Festa, J., Forbes, F., Geremia, E., Glocker, B., Golland, P., Guo, X., Hamamci, A., Iftekharuddin, K.M., Jena, R., John, N.M., Konukoglu, E., Lashkari, D., Mariz, J.A., Meier, R., Pereira, S., Precup, D., Price, S.J., Raviv, T.R., Reza, S.M.S., Ryan, M., Sarikaya, D., Schwartz, L., Shin, H.C., Shotton, J., Silva, C.A., Sousa, N., Subbanna, N.K., Szekely, G., Taylor, T.J., Thomas, O.M., Tustison, N.J., Unal, G., Vasseur, F., Wintermark, M., Ye, D.H., Zhao, L., Zhao, B., Zikic, D., Prastawa, M., Reyes, M., Leemput, K.V.: The multimodal brain tumor image segmentation benchmark (BRATS). IEEE Trans. Med. Imaging **34**, 1993–2024 (2015)
9. Pereira, S., Pinto, A., Alves, V., Silva, C.A.: Brain tumor segmentation using convolutional neural networks in MRI images. IEEE Trans. Med. Imaging **35**, 1240–1251 (2016)

10. Havaei, M., Davy, A., Warde-Farley, D., Biard, A., Courville, A., Bengio, Y., Pal, C., Jodoin, P.M., Larochelle, H.: Brain tumor segmentation with deep neural networks. Med. Image Anal. **35**, 18–31 (2017)
11. Kamnitsas, K., Ledig, C., Newcombe, V.F.J., Simpson, J.P., Kane, A.D., Menon, D.K., Rueckert, D., Glocker, B.: Efficient multi-scale 3D CNN with fully connected CRF for accurate brain lesion segmentation. Med. Image Anal. **36**, 61–78 (2017)
12. Long, J., Shelhamer, E., Darrell, T.: Fully convolutional networks for semantic segmentation. Presented at the Proceedings of the IEEE Conference on Computer Vision and Pattern Recognition (2015)
13. Arbelaez, P., Maire, M., Fowlkes, C., Malik, J.: Contour detection and hierarchical image segmentation. IEEE Trans. Pattern Anal. Mach. Intell. **33**, 898–916 (2011)
14. Nyúl, L.G., Udupa, J.K., Zhang, X.: New variants of a method of MRI scale standardization. IEEE Trans. Med. Imaging **19**, 143–150 (2000)
15. Simonyan, K., Zisserman, A.: Very deep convolutional networks for large-scale image recognition. arXiv:1409.1556 [cs] (2014)
16. Liaw, A., Wiener, M.: Classification and regression by randomForest. R News **2**, 18–22 (2002)
17. Vedaldi, A., Lenc, K.: MatConvNet: convolutional neural networks for MATLAB. In: Proceedings of the 23rd ACM International Conference on Multimedia, pp. 689–692. ACM, New York (2015)
18. Jia, Y., Shelhamer, E., Donahue, J., Karayev, S., Long, J., Girshick, R., Guadarrama, S., Darrell, T.: Caffe: convolutional architecture for fast feature embedding. In: Proceedings of the 22nd ACM International Conference on Multimedia, pp. 675–678. ACM, New York (2014)
19. Taormina, R.: MATLAB_ExtraTrees - File Exchange - MATLAB Central. http://uk.mathworks.com/matlabcentral/fileexchange/47372-rtaormina-matlab-extratrees
20. Bakas, S., Akbari, H., Sotiras, A., Bilello, M., Rozycki, M., Rozycki, M., Freymann, J., Farahani, K., Davatzikos, C.: Advancing the cancer genome atlas glioma MRI collections with expert segmentation labels and radiomic features. Nature Sci. Data (2017, in Press)
21. Bakas, S., Akbari, H., Sotiras, A., Bilello, M., Rozycki, M., Kirby, J., Freymann, J., Farahani, K., Davatzikos, C.: Segmentation labels and radiomic features for the pre-operative scans of the TCGA-GBM collection. The Cancer Imaging Archive (2017). https://doi.org/10.7937/K9/TCIA.2017.KLXWJJ1Q
22. Bakas, S., Akbari, H., Sotiras, A., Bilello, M., Rozycki, M., Kirby, J., Freymann, J., Farahani, K., Davatzikos, C.: Segmentation labels and radiomic features for the pre-operative scans of the TCGA-LGG collection. The Cancer Imaging Archive (2017). https://doi.org/10.7937/K9/TCIA.2017.GJQ7R0EF
23. Penn Imaging - Home. https://ipp.cbica.upenn.edu/
24. MICCAI-BraTS 2017 Leaderboard. https://www.cbica.upenn.edu/BraTS17/